https://doi.org/10.48048/tis.2025.9521

Antioxidant Potential of *Rhodiola Heterodonta* Extract: Activation of Nrf2 Pathway Via Integrative *In Vivo* and *In Silico* Studies

Azizbek Abdullaev[1*], Izzatullo Abdullaev[1], Anvarbek Bogbekov[3], Ulugbek Gayibov[1], Sirojiddin Omonturdiev[1], Sabina Gayibova[1], Muratbek Turahodjayev[2], Khaydarali Ruziboev[3] and Takhir Aripov[1]

[1]*A.S. Sadykov Institute of Bioorganic Chemistry of the Science Academy of Uzbekistan, Plant Cytoprotectors Laboratory, Tashkent, Uzbekistan*
[2]*Bioton LTD, Qibray, Argin, Uzbekistan*
[3]*National University of Uzbekistan named after Mirzo Ulugbek, University Street, Tashkent, Uzbekistan*

([*]Corresponding author's e-mail: dr.abdullaev.scientist@gmail.com)

Received: 14 December 2024, Revised: 11 January 2025, Accepted: 18 January 2025, Published: 15 March 2025

Abstract

This study investigates the antioxidant potential of *Rhodiola.h* extract using a combination of *in vivo* and *in silico* approaches. HPLC analysis was conducted to determine the phytochemical composition of the extract. *In vivo* assays demonstrated significant enzyme activation, with superoxide dismutase (SOD) activity increased by 63.07 ± 1.5 % and catalase activity increased by 58.7 ± 1.6 %. In addition, experiments evaluated malondialdehyde (MDA) levels, highlighting the extract's ability to reduce lipid peroxidation. Molecular docking studies revealed strong binding affinities of epigallocatechin (−7.09 kcal/mol), rosavin (−6.71 kcal/mol), and salidroside (−6.34 kcal/mol) with the Keap1 protein, a key regulator of the Nrf2 signaling pathway. Pharmacokinetic analysis showed high gastrointestinal absorption for salidroside and flavonoids, underscoring their bioavailability. These findings suggest that *R. heterodonta* extract holds promise for activating antioxidant response elements and mitigating oxidative stress-related damage.

Keywords: Antioxidant, Nrf2/Keap1/ARE signaling, HPLC, *Rhodiola.h*

Introduction

Oxidative stress, a state characterized by an imbalance between the production of reactive oxygen species (ROS) and the body's antioxidant defenses, is a critical factor in the progression of numerous chronic diseases, including cardiovascular, neurodegenerative diseases, and certain cancers [1,2]. Excessive ROS can lead to cellular damage through lipid peroxidation, DNA mutations, and protein degradation, ultimately impairing normal physiological functions. To counteract this, cells utilize a network of antioxidant defenses, one of the most significant being the Antioxidant Responsive Element (ARE) [3,4]. ARE activation is primarily regulated by the Keap1-Nrf2 pathway, in which the Kelch-like ECH-associated protein 1 (Keap1) serves as a sensor for oxidative stress. Under normal conditions, Keap1 binds to Nrf2 (nuclear factor erythroid 2–related factor 2) and promotes its degradation, maintaining low Nrf2 levels. However, in the presence of oxidative stress, Keap1 undergoes a conformational change, releasing Nrf2, which then translocates to the nucleus, binds to ARE, and induces the expression of a range of antioxidant enzymes that neutralize ROS and protect against cellular damage [5,6].

In traditional medicine, *Rhodiola.h* has long been valued for its adaptogenic and antioxidant properties, especially in managing stress, fatigue, and various health disorders [7]. This plant, belonging to the *Rhodiola.g*, is widely used across Central Asia, particularly in high-altitude regions where it is endemic.

Modern pharmacological studies are beginning to confirm the antioxidant potential of *Rhodiola.h*, revealing that it is rich in bioactive compounds—such as phenolic acids, flavonoids, and other polyphenols—that can modulate oxidative stress pathways, including the Keap1-Nrf2-ARE signaling cascade [8]. These compounds may influence Keap1's binding affinity for Nrf2, facilitating ARE activation and enhancing cellular defense mechanisms against oxidative stress [9,10].

The objective of the present study is to comprehensively evaluate the antioxidant potential of *Rhodiola.h* extract using a multifaceted approach. This includes *in vivo* assays to assess direct antioxidant activity and to observe physiological effects, and *in silico* analyses to understand molecular interactions, particularly with the Keap1-Nrf2 pathway [11,12]. High-performance liquid chromatography (HPLC) was also conducted to identify and quantify key bioactive compounds responsible for the plant's antioxidant effects. Through this integrated approach, the study aims to validate *Rhodiola.h* traditional uses and explore its potential as a therapeutic agent against oxidative stress-related diseases, with a particular focus on the modulation of the Keap1-Nrf2-ARE pathway [13,14].

Materials and methods

Plant material and extract preparation

The roots of *Rhodiola.h* were dried and finely ground, supplied by BIOTON Ltd. These plants were harvested in August 2020 from mountainous areas in Uzbekistan (Angren and Brichmulla regions, 1,200 - 1,400 m above sea level). The powdered samples were stored in desiccators until extraction. The extraction process utilized a Soxhlet apparatus with 40 % ethanol for 24 h [7]. Subsequently, the ethanol was removed using a rotary evaporator at +50 °C, and the extract was vacuum-concentrated until the moisture content was reduced to less than 15 %.

Drugs and reagents

Malondialdehyde (MDA) Assay Reagents: A lipid peroxidation assay kit, including thiobarbituric acid (TBA) and other necessary chemicals, was used to evaluate oxidative damage (Sigma-Aldrich, Catalog Number MAK085). Krebs-Ringer Solution: The Krebs-Ringer buffer is a physiological solution commonly used for maintaining cells or tissues in ex vivo experiments [8]. Its typical composition includes: Sodium chloride (NaCl): 118 mM, Potassium chloride (KCl): 4.7 mM, Calcium chloride dihydrate ($CaCl_2 \cdot 2H_2O$): 2.5 mM, Magnesium sulfate heptahydrate ($MgSO_4 \cdot 7H_2O$): 1.2 mM, Sodium bicarbonate ($NaHCO_3$): 25 mM, Glucose: 11 mM, Monopotassium phosphate (KH_2PO_4): 1.2 mM. Preparation: Dissolve the reagents in distilled water, adjust the pH to 7.4 using 1 N HCl or NaOH, and equilibrate the solution with 95 % O_2 and 5 % CO_2 gas for proper oxygenation. Alloxan: Used to induce diabetes *in vivo*, creating oxidative stress conditions for studying the protective effects of the extract. Keap1 Protein: Used for *in silico* docking studies to assess the binding affinities of phytochemicals with the key regulator of the Nrf2 antioxidant pathway. Catalase and Superoxide Dismutase (SOD) Enzymes: Utilized in enzyme inhibition assays to determine the antioxidant capacity of the extract. Pharmacokinetic Reagents: Computational tools were employed for pharmacokinetic and bioavailability analysis, assessing gastrointestinal absorption and other ADME (absorption, distribution, metabolism, and excretion) properties of the phytochemicals.

Units: The units used in this article are as follows: Milligrams per milliliter (mg/mL)**,** microliters (µl)**,** millimolar (mM)**,** grams (g)**,** kilocalories (kcal)**,** and percentage (%).

High-performance liquid chromatography (HPLC) analysis

Five g of *R. heterodonta* extract was precisely weighed and dissolved in 300 mL of distilled water. Subsequently, 50 mL of 70 % ethanol was added to the solution. This mixture was stirred for 1 h at a temperature of 40 - 50 °C, followed by 2 h at room temperature, and then centrifuged at 3,500 g for 20 min. The supernatant was collected, and the extraction process was repeated twice more[15,16]. The supernatants were filtered, combined, and the volume was adjusted to 100 mL using 70 % ethanol before HPLC analysis. The analysis utilized approximately 0.1 % trifluoroacetic acid, acetate buffer, and acetonitrile as solvents[17,18]. Chromatographic conditions for separation included the following setup: Agilent HPLC 1260 Infinity autosampler; Eclipse XDB-C18 column, 80 Å, 5 µm, 4.6×250 mm; detection at wavelengths of 247, 254, and

276 nm; a flow rate of 1 mL/min; and the eluent gradient as follows: Phosphate buffer at 95:5 from 0 - 5 min, 70:30 from 6 - 12 min, 50:50 from 12 - 13 min, and 95:5 from 13 - 15 min. The column temperature was maintained at 30 °C, with a sample injection volume of 10 µL. This experiment was conducted by Le laboratoire BotaniCERT in France.

Animal Experiments

All animal procedures adhered to the European Directive 2010/63/EU on the protection of animals used in scientific research (European Union, 2010). The study protocol received approval from the Animal Ethics Committee of the Institute of Bioorganic Chemistry, AS RUz (Protocol Number: 133/1a/h, dated August 4, 2014).

Experimental design

The experimental study was conducted at the Laboratory of Plant Cytoprotectors, Institute of Bioorganic Chemistry, Academy of Sciences of the Republic of Uzbekistan, in Tashkent. The study involved the use of *Rhodiola.h* extract, kindly provided by Bioton LLC. The extraction process was performed using a 70 % ethanol solution, followed by purification to remove ballast substances. The extract was then concentrated under vacuum and dried at a temperature not exceeding 60 °C to preserve its bioactive components.

The experimental animals used in this study were 30 non-linear white male rats, each weighing between 180 and 220 g. They were housed under standard vivarium conditions, with free access to food and water and exposure to natural light. Experimental diabetes mellitus (DM) was induced in the male rats through a single intraperitoneal injection of alloxan (Lachema, Czechoslovakia) at a dose of 140 mg/kg body weight. To facilitate the induction of diabetes, the male rats were fasted for 24 h before receiving the alloxan injection.

The male rats were divided into 3 experimental groups:

- Group 1: Healthy control animals.
- Group 2: Animals induced with diabetes by alloxan administration.
- Group 3: Diabetic male rats treated with *Rhodiola.h* extract (75 mg/kg) for 14 days, starting on the 14th day after diabetes induction, with administration every 2 - 3 days.

On the 15th day, the male rats were decapitated, and organs were harvested. The level of malondialdehyde (MDA), a marker of oxidative stress, was measured in organ homogenates from the heart, liver, kidneys, pancreas, small intestine, lungs, testicles, and brain. The MDA concentration was determined spectrophotometrically at 532 nm, using the molar extinction coefficient and the formula:

$$C_{MDA}=(\Delta D/0{,}156) \times 16.^{2} (1)$$

This method follows the protocol established by M. Uchiyama and M. Mihara. Statistical analysis of the data was performed using the Origin Pro Lab 8.5 software, with a sample size of n = 4 - 5 per group. This study aims to assess the potential antioxidant and cytoprotective properties of *Rhodiola.h* in a model of experimental diabetes mellitus.

Tissue preparation

Surgical procedures were carried out under sodium pentobarbital anesthesia, with all efforts made to minimize animal distress. The study involved white male rats with a body weight between 180 and 220 g [19].

In vivo antioxidant assays

Measurement of superoxide dismutase (SOD) activity

The activity of Superoxide Dismutase (SOD) was determined by measuring its ability to inhibit the reduction of nitroblue tetrazolium (NBT) by superoxide radicals. Heart tissue samples were homogenized in ice-cold phosphate buffer (50 mM, pH 7.4) and centrifuged at 10,000× g for 10 min at 4 °C to obtain the supernatant. In the assay, 50 µL of tissue supernatant was mixed with 50 mM phosphate buffer (pH 7.8), 0.1 mM EDTA, 13 mM L-methionine, 75 µM NBT, and 2 µM riboflavin. The reaction mixture was exposed to light for 10 min to induce superoxide generation. The absorbance was then measured at 560 nm using a spectrophotometer. One unit of SOD activity was defined as the amount of enzyme required to inhibit NBT reduction by 50 %. Results were expressed as units of SOD activity per mg of protein [20].

Measurement of catalase (CAT) activity

Catalase (CAT) activity was measured by assessing the decomposition of hydrogen peroxide (H_2O_2) spectrophotometrically. Tissue samples were homogenized in phosphate buffer (50 mM, pH 7.0) and centrifuged at 10,000× g for 10 min at 4 °C to obtain the supernatant. In the assay, 50 µL of tissue supernatant was added to a reaction mixture containing 50 mM phosphate buffer (pH 7.0) and freshly prepared 30 mM H_2O_2. The decrease in absorbance at 240 nm was monitored over 1 min, which reflects the breakdown of H_2O_2 by catalase. One unit of CAT activity was defined as the amount of enzyme required to decompose 1 µmol of H_2O_2 per min. Results were expressed as units of CAT activity per mg of protein [21].

Measurement of MDA in organs

The level of Thiobarbituric Acid Reactive Substances (TBARS), used as an indicator of Malondialdehyde (MDA) production and lipid peroxidation, was evaluated in tissue samples following the method of Heath and Packer. Briefly, 1 mL of tissue supernatant was combined with 4 mL of 20 % Trichloroacetic Acid (TCA) containing 0.5 % Thiobarbituric Acid (TBA) in tubes. The mixture was heated to 95 °C for 30 min, then allowed to cool before being centrifuged at 10,000× g for 10 min. The MDA-TBA adduct formed was quantified using a spectrophotometer at a wavelength of 532 nm [22].

In silico experiments

Molecular docking with KEAP1

To examine the binding interactions of the tested compounds with Keap1, molecular docking was carried out using a grid-based energy evaluation in the Autodock Vina program [24,25]. The crystal structure of Keap1 (PDB ID: 1X2R) was prepared as the docking receptor by adding polar hydrogen atoms and assigning Kollman charges. A specific grid box with a grid spacing of 0.375 Å was created around the receptor's binding site to encompass all key Keap1 residues. For each compound, the lowest binding energy (kcal/mol) was determined using the Lamarckian genetic algorithm, and these values were used to rank the compounds [26,27]. The binding interactions between Keap1 and each compound were visualized using PyMol and Discovery Studio 2018.

Analysing pharmacokinetics of Rhodiola.h extract

Screening for drug-likeness and toxicity allows for predicting whether a chemical may function effectively as an orally active compound [28,29]. To assess drug-likeness based on the Rule of Five and evaluate toxicity, the canonical SMILES notation for each ligand, obtained from PubChem, was entered into SwissADME, a publicly accessible online tool that does not require login credentials[30].

Statistical analysis

The results are presented as mean ± standard deviation (SD). Each assay was independently performed at least 3 times, and statistical analysis was conducted using the Student's t-test. Data for each treatment represent 3 independent replicates (3 and 6; $p < 0.05$, $p < 0.01$, and $p < 0.001$, respectively). Figures were created using OriginPro Lab 8.5 software.

Results and discussion

HPLC analysis results

Through HPLC analysis, several bioactive compounds were identified in the composition of *Rhodiola heterodonta*. Each of these compounds contributes to the plant's overall antioxidant and adaptogenic properties, as detailed below:

Firstly, gallic acid was identified, with a retention time (Tr) of 0.93 min. This compound is known for its strong antioxidant properties, helping to reduce oxidative stress in cells and protect their structural integrity [31]. The next identified compound is Rhodiocyanoside A, observed at a retention time of 1.26 min. This cyanogenic glycoside is characteristic of Rhodiola species and may enhance the plant's stress-resistance properties (**Figure 1**).

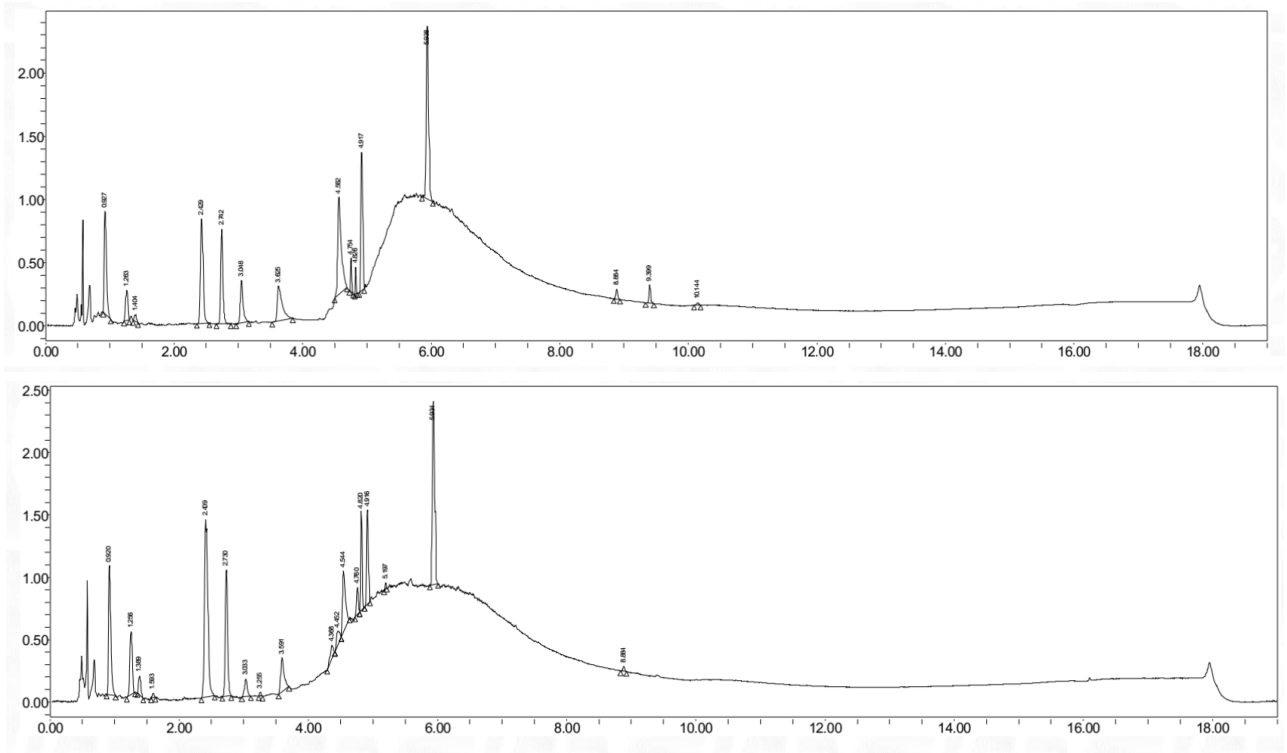

Figure 1 HPLC Chromatogram of Bioactive Compounds Identified in *Rhodiola.h* Identification of key bioactive compounds including gallic acid, Rhodiocyanoside A, salidroside, epigallocatechin (EGC), heterodontoside, viridoside and vanillin with their respective retention times.

Additionally, tyrosol derivatives were identified at retention times of 1.40 and 2.74 min. Tyrosol and its derivatives possess antioxidant and anti-inflammatory effects, which may support cardiovascular health and reduce neurodegenerative damage. At a retention time of 2.43 min, salidroside was detected. Salidroside is a key active component in *Rhodiola species*, known for its adaptogenic, anti-fatigue, and neuroprotective effects. Epigallocatechin (EGC) was detected at a retention time of 3.05 min. EGC belongs to the flavan-3-ol class and is recognized as a potent antioxidant. It supports cellular health and positively impacts the cardiovascular and nervous systems. At a retention time of 4.83 min, heterodontoside was identified [33,34]. This phenylpropanoid compound is unique to certain *Rhodiola species* and is known for its stress-relieving properties.

Subs.	Tr (UV)	% aire (rel)	UV (λmax)	[M+H]+ [M+Na]+	MS^2 (m/z)	Tentative identification	Structure confirmée ou hypothèse
C1	0,93	9,5	215, 271	171	171	Phenolic acid	Gallic acid
C2	1,26	3,0	208	260	260, 282	Cyanogenic glycoside	Rhodiocyanoside A
C3	1,40	0,7	220, 269	-	121, 611	Phenylpropane	Tyrosol derivative
C5	2,43	12,7	221, 275	323	121, 323	Phenylpropane	Salidroside
C6	2,74	10,0	221, 276	-	121	Phenylpropane	Tyrosol
C7	3,05	5,4	206, 270	307	307	Flavan-3-ol	Epigallocatechin (EGC)
C9	3,63	7,6	208, 272	763	763	Flavan-3-ol	Dimer EGC-EGCG
C12	4,56	15,8	208, 273	459	459	Flavan-3-ol	Epigallocatechin gallate (EGCG)
C13	4,75	1,7	221, 275	-	135	Phenylpropane	Tyrosol methyl ether derivative
C15	4,83	1,1	222, 275	-	135	Phenylpropane	Heterodontoside
C16	4,92	11,5	222, 275	-	135, 337, 353, 648	Phenylpropane	Viridoside
C18	5,94	18,8	227, 275	-	135	Phenylpropane	Tyrosol methyl ether
C20	8,88	0,9	220, 273	-	-	Flavan-3-ol	EGCG derivative
C21	9,40	1,1	218, 261	-	133	Phenylpropane	4-methoxyphenylacetaldehyde (supposition)
C22	10,1	0,2	195	-	-	Unknown	-

Subs.	Tr (UV)	% aire (rel)	UV (λmax)	[M+H]+ [M+Na]+	MS^2 (m/z)	Tentative identification	Structure confirmée ou hypothèse
C1	0,93	10,4	215, 271	171	171	Phenolic acid	Gallic acid
C2	1,26	5,6	208	260	260, 282	Cyanogenic glycoside	Rhodiocyanoside A
C3	1,40	1,6	220, 269	-	121, 611	Phenylpropane	Tyrosol derivative
C4	1,59	0,4	-	-	-	Phenylpropane	Tyrosol derivative
C5	2,43	22,8	221, 275	323	121, 323	Phenylpropane	Salidroside
C6	2,74	11,8	221, 276	-	121	Phenylpropane	Tyrosol
C7	3,05	1,8	206, 270	307	307	Flavan-3-ol	Epigallocatechin (EGC)
C8	3,26	0,2	224, 272	-	-	Phenylpropane	Tyrosol derivative
C9	3,63	4,3	208, 272	763	763	Flavan-3-ol	Dimer EGC-EGCG
C10	4,37	1,5	204, 280	-	-	Phenylpropane	-
C11	4,45	1,6	208, 273	-	-	Flavan-3-ol	EGCG derivative
C12	4,56	6,6	208, 273	459	459	Flavan-3-ol	Epigallocatechin gallate (EGCG)
C14	4,75	1,7	221, 275	-	-	Flavan-3-ol	EGCG derivative
C15	4,83	6,0	222, 275	-	135	Phenylpropane	Heterodontoside
C16	4,92	6,4	222, 275	-	135, 337, 353, 648	Phenylpropane	Viridoside
C17	5,20	0,3	208, 282	-	-	Phenylpropane	Tyrosol methyl ether derivative
C18	5,94	16,8	227, 275	-	135	Phenylpropane	Tyrosol methyl ether
C20	8,88	0,3	220, 273	-	-	Flavan-3-ol	EGCG derivative

Figure 2 HPLC Analysis of *Rhodiola.h* extract: Key Compounds and Retention Times Chromatographic profile illustrating the retention times of major bioactive compounds detected in *Rhodiola.h*.

Another compound identified at a retention time of 4.92 min was viridoside, a phenylpropanoid with antioxidant and neuroprotective properties, though its full therapeutic potential is still under research. Epigallocatechin gallate (EGCG) derivatives were also detected, further strengthening the plant's antioxidant profile. EGCG is widely recognized for its cardioprotective, anti-inflammatory, and anticancer effects. Lastly, a compound tentatively identified as 4-methoxyphenylacetaldehyde was observed at an approximate retention time of 9.4 min. This aldehyde derivative may contribute to the plant's bioactivity or aroma profile (**Figure 2**). These findings illustrate the retention times of key compounds identified within *Rhodiola.h*, highlighting its potent antioxidant, adaptogenic, and stress-resistance qualities. The data support the plant's traditional medicinal uses with a scientific basis [35,36].

***In vivo* studies of *Rhodiola.h* extract for antioxidant activity**

The Table illustrates MDA levels in various organs, comparing intact controls, diabetic subjects, and those treated with *Rhodiola.h*. Under normal (intact) conditions, MDA levels were consistent across organs, ranging from 8.44 ± 0.15 in the testes to 12.71 ± 0.36 in the small intestine, reflecting low oxidative stress in healthy tissue [35]. However, diabetes markedly elevated MDA concentrations in all examined organs, with the highest levels observed in the small intestine (19.65 ± 0.36) and kidneys (18.45 ± 0.69), indicating extensive lipid peroxidation due to hyperglycemia-induced oxidative stress (**Table 1**).

Table 1 Malondialdehyde (MDA) levels in various organs of experimental rat.

Organs	Brain	Heart	Kidneys	Small intestine	Pancreas	Testes	Liver	Lungs
Intact	11.02 ± 0.42	10.89 ± 0.17	10.08 ± 0.47	11.94 ± 0.25	9.04 ± 0.29	9.53 ± 0.21	10.73 ± 0.41	11.07 ± 0.22
Alloxan induced - Diabetes	17.95 ± 0.51	18.01 ± 0.25	19.03 ± 0.74	19.65 ± 0.36	16.87 ± 0.54	18.12 ± 0.45	16.92 ± 1.12	19.04 ± 0.35
Rhodiola heterodonta	11.28 ± 1.10	14.29 ± 0.78	12.68 ± 1.39	11.86 ± 0.11	12.64 ± 0.42	11.82 ± 0.87	12.44 ± 0.79	12.68 ± 1.39

Treatment with *Rhodiola.h* showed a significant reduction in MDA levels compared to diabetic controls, although the values did not return to the baseline seen in intact subjects. For example, in the brain, MDA levels decreased from 18.22 ± 0.21 in diabetic conditions to 11.28 ± 1.10 with treatment, approaching the intact level of 10.94 ± 0.42. Similar trends were observed in other organs, such as the heart and lungs, where treatment resulted in reductions to 14.29 ± 0.78 and 12.68 ± 1.39, respectively, compared to diabetic levels of 17.43 ± 1.02 and 18.18 ± 0.42 (**Table 1**) [36].

SOD and catalase activity of Rhodiola.h extract

The SOD experiments illustrate the effect of diabetes and treatment with *Rhodiola.h* extract on superoxide dismutase (SOD) activity in rat liver homogenate. SOD activity is presented as the percentage inhibition of the reduction of nitroblue tetrazolium (NBT) by superoxide anions, reflecting the enzyme's ability to neutralize reactive oxygen species (ROS) and protect cells from oxidative damage [31].

In the control group (intact, healthy male rats), SOD activity is high, with an inhibition level of approximately 94.33 ± 1.2 %. This high level of activity represents the liver's normal antioxidant defense, which efficiently counters oxidative stress in healthy cells. The intact group sets a baseline for comparison, showing the liver's typical enzymatic response without the influence of diabetes or treatment.

In contrast, male rats in the alloxan-induced diabetic group exhibit a marked reduction in SOD activity, with an inhibition percentage of about 63.07 ± 1.5 %. The decline in SOD activity in this group suggests that diabetes significantly compromises the liver's antioxidant defense. Alloxan-induced diabetes is known to increase oxidative stress, leading to higher levels of ROS that can overwhelm the antioxidant system, resulting in diminished SOD activity. This reduction implies that diabetes severely impacts the liver's capacity to manage oxidative stress, possibly contributing to cellular damage and further complications associated with diabetic conditions [32].

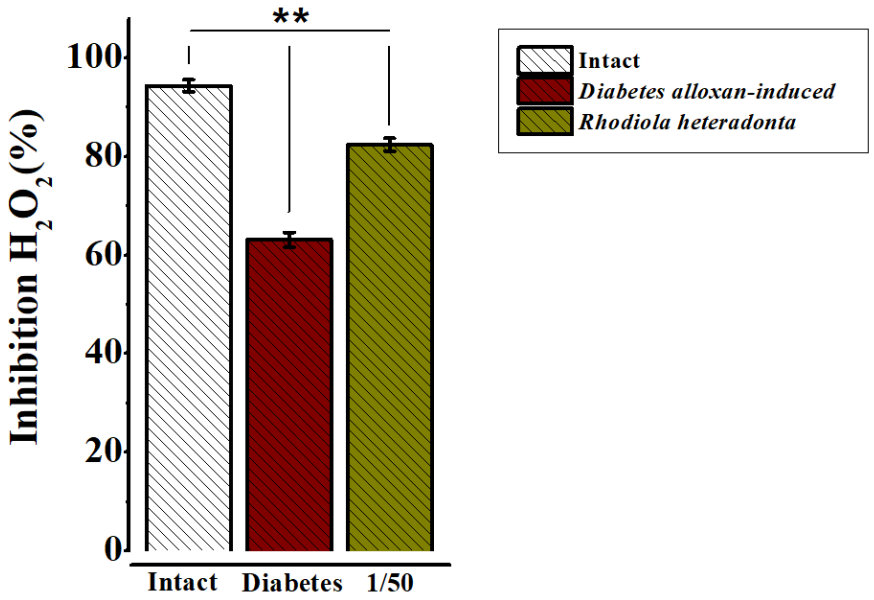

Figure 3 Illustration of the effect of diabetes and treatment with Rhodiola.h extract on superoxide dismutase (SOD) activity in rat liver homogenate $p < 0.01^{**}$ n = 4 - 6.

Male Rats treated with *Rhodiola.h* extract at a 1/50 dilution demonstrate a notable increase in SOD activity compared to the diabetic group, reaching an inhibition level of approximately 82.33 ± 1.3 %. Although this level does not fully restore SOD activity to that of the intact group, it significantly improves antioxidant activity in diabetic male rats (**Figure 3**). The increase in SOD activity suggests that *Rhodiola.h* extract may have protective or restorative effects on antioxidant enzymes under diabetic conditions. This improvement indicates that the extract likely provides beneficial bioactive compounds that counteract the oxidative damage caused by diabetes, partially enhancing the liver's natural defense mechanisms against ROS. H_2O_2

Catalase activity of the extract Rhodiola.h

The presented Figure shows the effect of alloxan-induced diabetes and treatment with *Rhodiola.h* extract on catalase activity in rat liver homogenates, expressed as the percentage of hydrogen peroxide (H_2O_2) inhibition. In the intact group, catalase activity resulted in 57.4 % inhibition, indicating normal enzymatic activity in healthy male rats. In contrast, the alloxan-induced diabetic group displayed a significant reduction in catalase activity, with only 32.6 % inhibition, suggesting that oxidative stress and impaired antioxidant defense were present due to the diabetic condition. However, treatment with *Rhodiola.h* extract (1/50 dilution) significantly increased catalase activity, restoring it to 58.7 % inhibition, comparable to the intact group. This indicates that *Rhodiola.h* has a potential protective or restorative effect on liver antioxidant function under diabetic conditions, possibly through the enhancement of antioxidant enzyme activity such as catalase and superoxide dismutase (SOD), which are key players in the defense against oxidative stress [33,34].

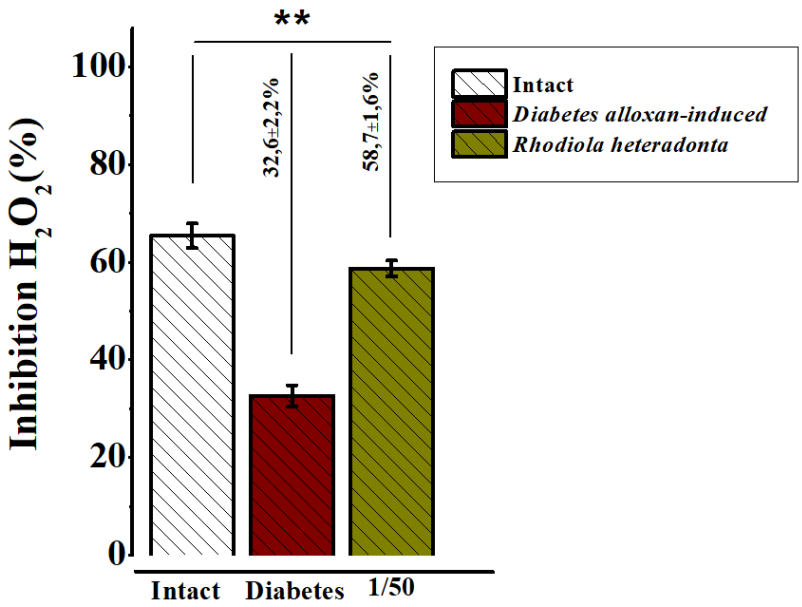

Figure 4 Catalase activity in the liver homogenate of rats with alloxan-induced diabetes was 32.6 ± 2.2 %, compared to 65.4 ± 2.5 % in the intact control group ($p < 0.01$). Treatment with Rhodiola.h extract (1/50 dilution) restored catalase activity to 58.7 ± 1.6 % ($p < 0.01$ vs. diabetes group).

These findings suggest that *Rhodiola.h* possesses antioxidant properties capable of mitigating lipid peroxidation and oxidative stress in diabetes-induced conditions. This highlights its potential therapeutic application in protecting organs from oxidative damage associated with hyperglycemia. However, the variability in response across different organs warrants further investigation to elucidate the mechanisms underlying its organ-specific effects [36].

***In silico* molecular docking and pharmacokinetics**

Interaction of derivates of rhodiola.h with keap1

Docking studies between the Derivates and Nrf2 successfully replicated the known binding conformations in the Keap1-Nrf2 complex (PDB: 1X2R), validating the Keap1 model's reliability for calculating binding free energies. Results from the docking analysis ranked the binding affinities of the derivates of Rhodiola.h with Keap1 in descending order as follows: vanillin > flavan > rhadiocyanoside > salidroside > rosavin > epigalocatechin (**Table 2**). The colors in the 2D and 3D representations in (**Figure 5**) dark green, light green, orange, pink, red, and cyan—represent interactions including hydrogen bonds, van der Waals forces, carbon-hydrogen bonds, and Pi-cation interactions, respectively (**Figure 5**) [25]. Based on this data, the derivates of Rhodiola.h extract is classified into weak agonists (vanillin, rhadiocyanoside A, flavan) and strong agonists (salidroside, rosavin and epigallocatechin), with activation potency largely corresponding to binding affinities for Keap1.

"DiscoveryStudio" depict the molecular docking interactions between a rosavin (ligand) and the Keap1 protein, highlighting key amino acid residues and the types of bonds involved. In the first Figure, the ligand interacts with several residues, including VAL418, VAL420, VAL512, VAL465, VAL466, VAL467, VAL608, ALA368, ALA465, ALA467, GLY419, GLY561, CYS513, and LEU514 and LEU515. The interactions consist of van der Waals forces, conventional hydrogen bonds, carbon-hydrogen bonds, and Pi-Alkyl interactions. One unfavorable interaction is observed with VAL465, indicating slight steric or electronic hindrance. The ligand is well-positioned in the binding pocket, with multiple hydrogen bonds stabilizing its orientation, though the unfavorable interaction at VAL465 suggests a potential area for improvement in ligand design. Another docking configuration, where the salidroside (ligand) interacts with residues such as GLY419, ALA607, VAL512, VAL467, VAL608, and THR560. The interactions include conventional hydrogen bonds, carbon-hydrogen bonds, and a Pi-Sigma interaction involving the

aromatic ring. These interactions contribute to the ligand's stability and affinity within the Keap1 binding site [26]. With regards to interactions of epigallocatechin between compound and various amino acid residues within a binding site. The green lines indicate van der Waals interactions with residues like VAL 369, VAL 418, and VAL 465, showing close but non-bonded contact points. Red dashed lines represent hydrogen bonds, including those with VAL 512, CYS 513, and ALA 420, which enhance binding specificity. Pink lines highlight alkyl and Pi-alkyl interactions with hydrophobic residues such as ALA 466 and VAL 561. Together, these interactions suggest a stable binding conformation, supported by a mix of van der Waals forces, hydrogen bonding, and hydrophobic interactions (**Figure 5**) [27].

Table 2 Structural depictions of the Keap1-ligand complex.

Compounds of rhodiola heteradonta	Chemical structures	Affinity (kcal/mol)	Agonist potency
Rosavin	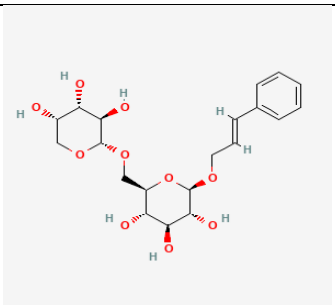	−6.71 kcal/mol	Strong agonist
Rhadiocyanoside	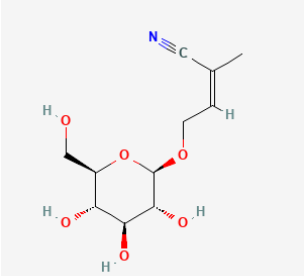	−5.91 kcal/mol	Weak agonist
Salidroside	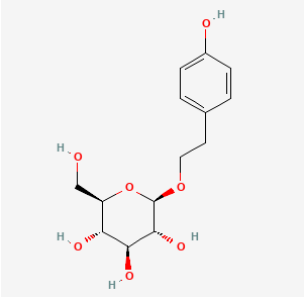	−6.34 kcal/mol	Weak agonist
Epigalochetcin	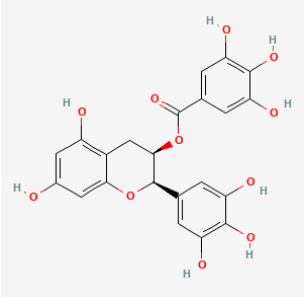	−7.09 kcal/mol	Strong agonist

Compounds of rhodiola heteradonta	Chemical structures	Affinity (kcal/mol)	Agonist potency
Flavan	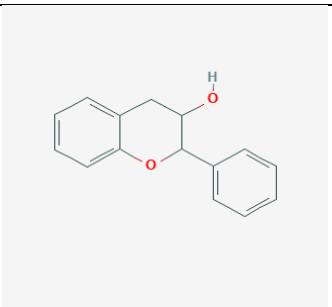	−6.26 kcal/mol	Weak agonist
Vanillin	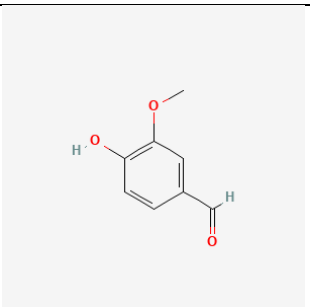	−4.38 kcal/mol	Weak agonist

Molecular interactions (3D)	Interaction with amino acids (2D)
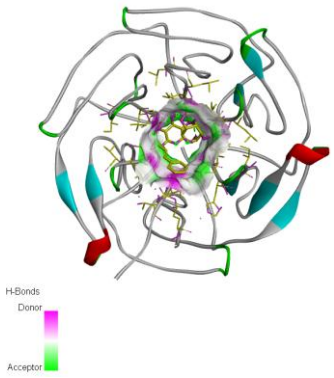 **Rosavin**	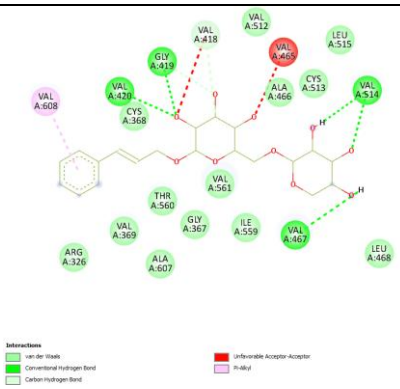
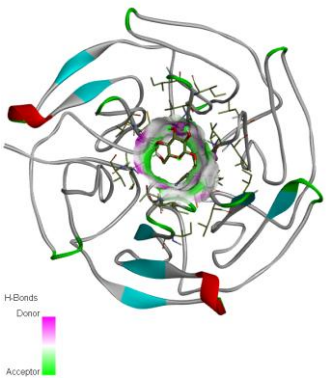 **Rhadiocyanoside A**	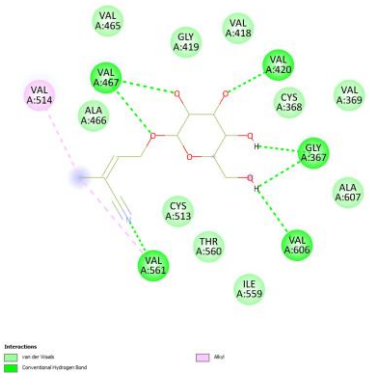

Molecular interactions (3D)	Interaction with amino acids (2D)
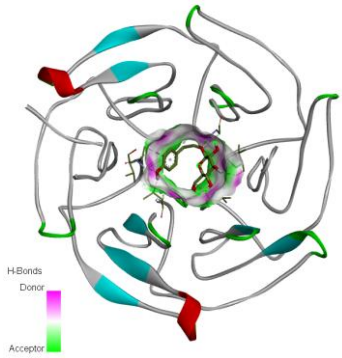 **Salidroside**	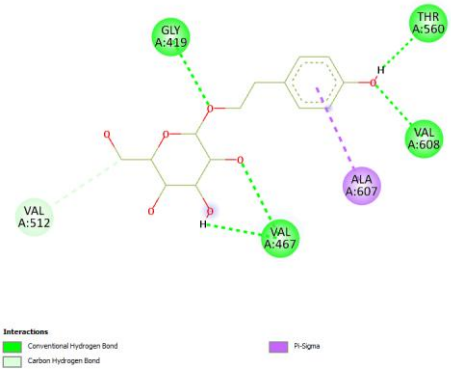
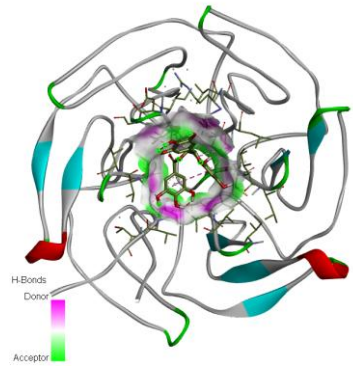 **Epigallocatechin gallate**	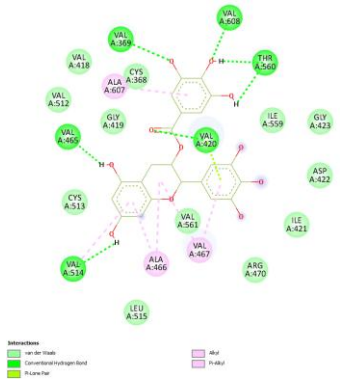
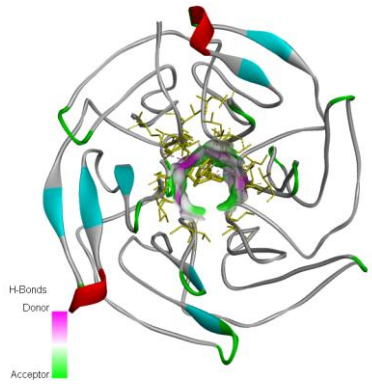 **Flavan**	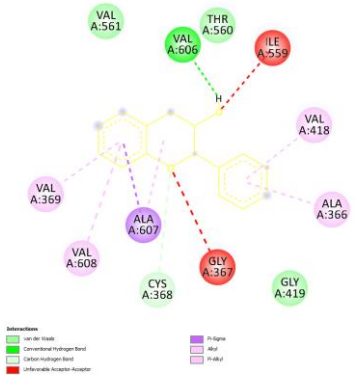

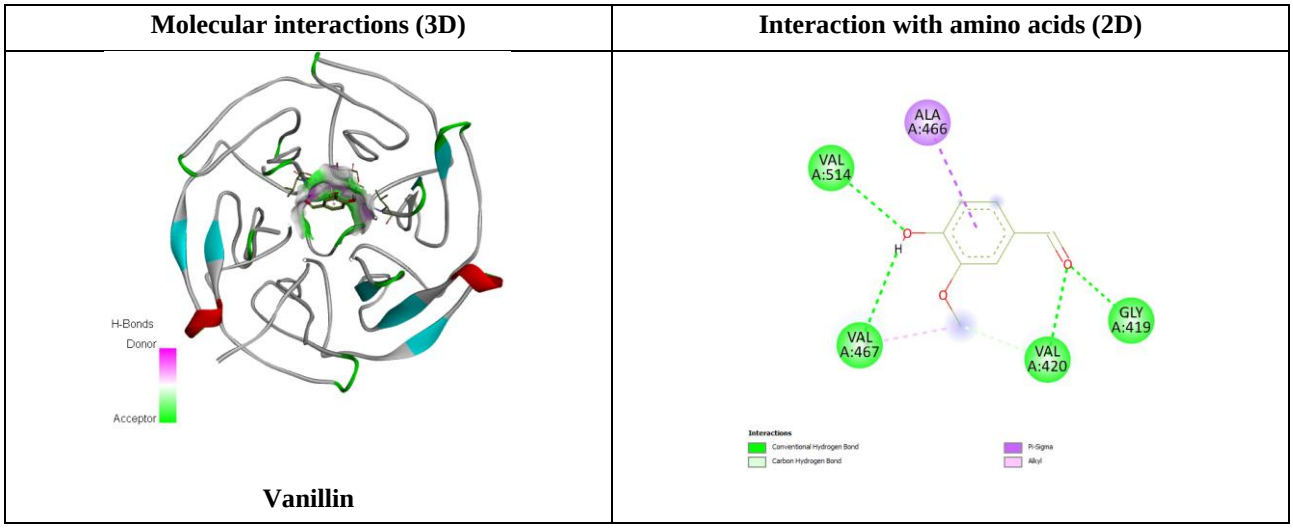

Figure 5 Structural depiction of the Keap1-ligand complex in a strong agonist configuration. Panels display the "molecular interactions (3D)", while panels "interaction with amino acids" illustrate their corresponding (2D) structures.

In silico pharmacokinetic properties

As biological and chemical data expand rapidly, evaluating the physicochemical and ADME (Absorption, Distribution, Metabolism, and Excretion) properties has become crucial in identifying bioactive compounds from traditional plants [28,29]. To assess the bioavailability of phytochemicals, key factors such as pharmacokinetics, bioavailability, drug-likeness, and alignment with medicinal chemistry standards were examined following "Lipinski's Rule of Five". This rule states that an ideal compound should have a molecular weight below 500 Dalton, no more than 5 hydrogen bond donors, a maximum of ten hydrogen bond acceptors, and a LogP (partition coefficient) less than 5. SwissADME analysis (**Table 3**) showed that Rhadiocyanoside, Salidroside, and Flavan meet all these criteria without any violations, suggesting good drug-like potential. Compounds with more than 2 violations are generally considered poor candidates for oral bioavailability, making these 3 flavonoids promising for further research [30].

Table 3 That summarizes the predicted ADME profiles for each compound, including water solubility, pharmacokinetics, bioavailability, drug-likeness, and medicinal chemistry properties.

Compounds	Water solubility		Pharmacokinetics			Druglikeness				Medicinal chemistry	
	Log S (ESOL)	Log S (Ali)	G_i absorption	BBB permeant	Log K_p	Lipinski	Ghose	Muegge	Bioavailability score	PAINS	Leadikenes
Rosavin	−4	−3	Low	No	low	Yes	No	No	0.11	0	No
Rhadiocyanoside	−0.04	−0.26	Low	No	−9.17cm/s	Yes	No	Yes	0.55	0	Yes
Salidroside	−0.92	−0.97	High	No	−8.88 cm/s	Yes	No	Yes	0.55	0	Yes
Epigalochetcin	−3.56	−4.91	Low	No	−8.27 cm/s	No	Yes	No	0.17	1	No
Flavan	−3.49	−3.12	High	Yes	−5.56 cm/s	Yes	Yes	Yes	0.55	0	No
Vanilin											

Skin permeability (Kp, cm/s) was analyzed to assess skin absorption potential, where more negative logKp values indicate lower skin absorption. All tested compounds have Kp values ranging from − 5.56 to −9.17, indicating low skin permeability. Furthermore, factors such as blood-brain barrier (BBB) permeability and gastrointestinal (GI) absorption were evaluated to better understand each compound's distribution and absorption. The SwissADME analysis reveals that all tested compounds have GI absorption, with salidroside and flavan displaying particularly favorable results. Overall, these ADME predictions and physicochemical

assessments indicate that naringenin, Flavan, and Salidroside may serve as better candidates for further investigation compared to other tested compounds.

Discussions

Significance of *in vivo* antioxidant activity

The *in vivo* analysis demonstrated that *Rhodiola.h* extract exhibits significant antioxidant activity through the enhancement of key enzymatic systems. Superoxide dismutase (SOD) activity increased by 63.07 ± 1.5%, and catalase activity was elevated by 58.7 ± 1.6 %. These findings highlight the extract's ability to modulate enzymatic activity, suggesting its potential in combating reactive oxygen species (ROS). Both SOD and catalase play critical roles in cellular antioxidant defense by mitigating oxidative damage caused by superoxide radicals and hydrogen peroxide, respectively. The increase in activity observed in this study indicates that *R. heterodonta* could help restore redox balance by enhancing enzymatic antioxidant pathways, making it a promising candidate for antioxidant therapies.

The *in vivo* experiments, using malondialdehyde (MDA) as a biomarker, demonstrated the extract's capacity to reduce lipid peroxidation, a key indicator of oxidative stress. The reduction in MDA levels underscores the therapeutic potential of *Rhodiola.h* extract in mitigating oxidative damage, particularly under pathological conditions such as diabetes. The use of alloxan to induce diabetes in the experimental model was instrumental, as alloxan-mediated oxidative stress disrupts antioxidant defense systems, including SOD and catalase. By challenging the antioxidant response system, alloxan-induced diabetes allowed us to investigate the protective effects of *Rhodiola.h* in conditions of elevated ROS. The observed reduction in MDA levels suggests that the extract could be effective in preventing oxidative stress-associated complications in diabetic models, potentially by modulating lipid peroxidation and preserving cell integrity.

Molecular insights from docking and pharmacokinetics

Molecular docking studies provided deeper insights into the interaction between *Rhodiola.h* bioactive compounds and Keap1 protein, a key regulator of the Nrf2 antioxidant pathway. Epigallocatechin exhibited the strongest binding affinity (− 7.09 kcal/mol), followed by rosavin (−6.71 kcal/mol) and salidroside (−6.34 kcal/mol). These compounds, acting as strong agonists, likely interfere with the Keap1-Nrf2 interaction, thereby activating Nrf2 and enhancing the expression of antioxidant-responsive elements. Weaker agonists such as flavan, rhadiocyanoside, and vanillin also demonstrated binding but with lower affinities, suggesting that they may have auxiliary roles in modulating antioxidant pathways.

Pharmacokinetic analysis revealed favorable gastrointestinal (GI) absorption for salidroside and flavan, supporting their bioavailability and therapeutic potential *in vivo*. High GI absorption ensures that these compounds can effectively reach systemic circulation and exert their biological effects, enhancing the extract's viability as a therapeutic agent for managing oxidative stress-related diseases.

Rationale for using alloxan

Alloxan was used in the experimental model to induce diabetes because of its well-established role in generating ROS and disrupting antioxidant defenses. Alloxan selectively targets pancreatic β-cells, leading to hyperglycemia and increased oxidative stress, which can significantly impair antioxidant enzymes like SOD and catalase. By utilizing this model, we aimed to mimic diabetic oxidative stress conditions to evaluate the efficacy of *Rhodiola.h* extract in restoring antioxidant balance. The significant reduction in MDA levels and the observed modulation of SOD and catalase activities in alloxan-treated models highlight the extract's potential to mitigate oxidative stress under diabetic conditions.

Conclusions

This study highlights the significant potential of *Rhodiola.h* extract as an activator of antioxidant responses, particularly in conditions of oxidative stress induced by diabetes. The extract demonstrated strong antioxidant properties by modulating enzymatic activity, as evidenced by the inhibition of SOD and catalase. *In vivo* experiments further confirmed its efficacy, with reduced malondialdehyde (MDA) levels indicating decreased lipid peroxidation and oxidative damage. Molecular docking studies revealed high binding affinities of key bioactive compounds, such as

epigallocatechin, rosavin, and salidroside, with Keap1 protein, suggesting their role in activating the Nrf2 antioxidant pathway. The favorable pharmacokinetic profiles, including high gastrointestinal absorption for salidroside and flavan, further support the therapeutic viability of the extract. The integration of *in vivo* and *in silico* approaches provided a comprehensive evaluation of the extract's antioxidant potential, showcasing its relevance as a multifaceted therapeutic agent. These findings lay the groundwork for future research and clinical investigations to explore the efficacy of *Rhodiola.h* in managing oxidative stress-related conditions, particularly in diabetes and other chronic diseases.

Acknowledgements

Izzatullo Ziyoyiddin o'g'li Abdullaev: Conducted molecular docking studies and prepared the initial draft of the manuscript. Azizbek Akbar o'g'li Abdullaev: Performed *in vivo* experiments and contributed to the data analysis. Anvarbek Ilhombek o'g'li Bogbekov: Assisted in molecular docking studies and provided technical support for computational analyses. Ulugbek Gapparjanovich Gayibov: Supervised and guided the molecular docking studies. Sirojiddin Zoirovich Omonturdiev: Supervised *in vivo* experiments and provided critical review of experimental designs. Sabina Narimanovna Gayibova: Supervised *in vivo* experiments and ensured the accuracy of biochemical assays. Takhir Fatikhovich Aripov: Provided overall supervision of the project, contributed to conceptualization, and critically reviewed the manuscript.

Funding

Funded by the Innovative Development Agency under the Ministry of Higher Education, Science and Innovation of the Republic of Uzbekistan under the number FL-8323102109 "Potential medicinal plants of Uzbekistan with adaptogenic effects and their molecular, cellular and therapeutic effects mechanisms" project

References

[1] OS Zoirovich, AIZ Ugli, ID Raxmatillayevich, ML Umarjonovich1, ZM Ravshanovna, GS Narimanovna, GU Gapparjanovich and AT Fatikhovich. The effect of Ajuga Turkestánica on the rat aortic smooth muscle ion channels. *Biomedical and Pharmacology Journal* 2024; **17(2)**, 1213-1222.

[2] AA Abdullaev, DR Inamjanov, DS Abduazimova, SZ Omonturdiyed, UG Gayibov, SN Gayibova and TF Aripov. *Silybum Marianum's* impact on physiological alterations and oxidative stress in diabetic rats. *Biomedical and Pharmacology Journal* 2024; **17(2)**, 1291-1300.

[3] T Guan, N Li, X Xu, D Xing, B Wang, L Xiao, W Yang, G Chu, A Yusuf, J Zhang and W Yue. Involvement of the Keap1-Nrf2-ARE pathway in the antioxidant activity of sinomenine. *Archives of Biochemistry and Biophysics* 2024; **753**, 109928.

[4] Izzatullo Ziyoyiddin o`g`li Abdullaev, Ulugbek Gapparjanovich Gayibov, Sirojiddin Zoirovich Omonturdiev, Sobirova Fotima Azamjonovna, Sabina Narimanovna Gayibova, Takhir Fatikhovich Aripov. Molecular pathways in cardiovascular disease under hypoxia: Mechanisms, biomarkers, and therapeutic targets[J]. The Journal of Biomedical Research. DOI: 10.7555/JBR.38.20240387

[5] E Bhakkiyalakshmi, K Dineshkumar, S Karthik, D Sireesh, W Hopper, R Paulmurugan and KM Ramkumar. Pterostilbene-mediated Nrf2 activation: Mechanistic insights on Keap1: Nrf2 interface. *Bioorganic & Medicinal Chemistry* 2016; **24(16)**, 3378-3386.

[6] MM Khalaf, SM Hassan, AM Sayed and AM Abo-Youssef. Ameliorate impacts of scopoletin against vancomycin-induced intoxication in rat model through modulation of Keap1-Nrf2/HO-1 and IkappaBalpha-P65 NF-kappaB/P38 MAPK signaling pathways: molecular study, molecular docking evidence and network pharmacology analysis. *International Immunopharmacology* 2022; **102**, 108382.

[7] MR Zaripova, SN Gayibova, RR Makhmudov, AA Mamadrahimov, NI Vypova, UG Gayibov, SM Miralimova and TF Aripov. Characterization of rhodiola heterodonta (crassulaceae): Phytocomposition, antioxidant and antihyperglycemic activities. *Preventive Nutrition and Food Science* 2024; **29(2)**, 135-145.

[8] H Lv, C Zhu, W Wei, X Lv, Q Yu, X Deng and X Ci. Enhanced Keap1-Nrf2/Trx-1 axis by daphnetin protects against oxidative stress-driven hepatotoxicity via inhibiting ASK1/JNK and Txnip/NLRP3 inflammasome activation. *Phytomedicine* 2020; **71**, 153241.

[9] L Ren, H Luo, J Zhao, S Huang, J Zhang and C Shao. An integrated *in vitro/in silico* approach to assess the anti-androgenic potency of isobavachin. *Food and Chemical Toxicology* 2023; **176**, 113764.

[10] Y Liang, Q Jiang, Y Gong, Y Yu, H Zou, J Zhao, T Zhang and J Zhang. *In vitro* and *in silico* assessment of endocrine disrupting effects of food contaminants through pregnane X receptor. *Food and Chemical Toxicology* 2023; **175**, 113711.

[11] S Liu, J Pi and Q Zhang. Signal amplification in the KEAP1-NRF2-ARE antioxidant response pathway. *Redox Biology* 2022; **54**, 102389.

[12] L Ren, J Zhang and T Zhang. Immunomodulatory activities of polysaccharides from *Ganoderma* on immune effector cells - science direct. *Food Chemistry* 2020; **340**, 127933.

[13] E Crisman, P Duarte, E Dauden, A Cuadrado, MI Rodriguez-Franco, MG Lopez and R Leon. KEAP1-NRF2 protein–protein interaction inhibitors: Design, pharmacological properties and therapeutic potential. *Medicinal Research Reviews* 2023; **43(1)**, 237-287.

[14] L He, P Huan, J Xu, Y Chen, L Zhang, J Wang, L Wang and Z Jin. Hedysarum polysaccharide alleviates oxidative stress to protect against diabetic peripheral neuropathy via modulation of the keap1/Nrf2 signaling pathway. *Journal of Chemical Neuroanatomy* 2022; **126**, 102182.

[15] Y Qi, S Fu, D Pei, Q Fang, W Xin, X Yuan, Y Cao, Q Shu, X Mi and F Luo. Luteolin attenuated cisplatin- induced cardiac dysfunction and oxidative stress via modulation of Keap1/Nrf2 signaling pathway. *Free Radical Research* 2022; **56(2)**, 209-221.

[16] A Chakkittukandiyil, DV Sajini, A Karuppaiah and D Selvaraj. The principal molecular mechanisms behind the activation of Keap1/Nrf2/ARE pathway leading to neuroprotective action in Parkinson's disease. *Neurochemistry International* 2022; **156**, 105325.

[17] O Gaibullayeva, A Islomov, D Abdugafurova, B Elmurodov, B Mirsalixov, L Mahmudov, I Adullaev, K Baratov, S Omonturdiev and S Sa'dullayeva. Inula helenium l. root extract in sunflower oil: Determination of its content of water-soluble vitamins and immunity-promoting effect. *Biomedical and Pharmacology Journal* 2024; **17(4)**, 2729-2737.

[18] Thermo Fisher Scientific: HPLC Basics Thermo Fisher Scientific - US. *Detailed explanation of HPLC operation, including isocratic and gradient methods, and applications in various industries*. Thermo Fisher Scientific: HPLC Basics Thermo Fisher Scientific - US, Massachusetts, 2025.

[19] AQQ Azimova, AX Islomov, SA Maulyanov, DG Abdugafurova, LU Mahmudov, IZO Abdullaev, A Ishmuratova, SQQ Siddikova and IR Askarov. Determination of vitamins and pharmacological properties of vitis vinifera L. Plant fruit part (mixed varieties) syrup-honey. *Biomedical and Pharmacology Journal* 2024; **17(4)**, 2779-2786.

[20] Inomjonov, D., Abdullaev,I., Omonturdiev, S., Abdullaev, A., Maxmudov, L., Zaripova, M., Abdullayeva, M., Abduazimova, D., Menglieva, S., Gayibova, S., Sadbarxon, M., Gayibov, U., & Aripov, T. (2025). In Vitro and In Vivo Studies of Crategus and Inula helenium extracts: Their Effects on Rat Blood Pressure. Trends in Sciences, **22(3)**, 9158.

[21] UG Gayibov, SN Gayibova, HM Karimjonov, AA Abdullaev, DS Abduazimova, RN Rakhimov, HS Ruziboev, MA Xolmirzayeva, AE Zaynabiddinov and TF Aripov. Antioxidant and cardioprotective properties of polyphenolic plant extract of Rhus glabra L. *Plant Science Today* 2024; **11(3)**, 655-662.

[22] C Beauchamp and I Fridovich. Superoxide dismutase: Improved assays and an assay applicable to acrylamide gels. *Analytical Biochemistry* 1971; **44(1)**, 276-287.

[23] RF Beers and IW Sizer. A spectrophotometric method for measuring the breakdown of hydrogen peroxide by catalase. *Journal of Biological Chemistry* 1952; **195(1)**, 133-140.

[24] SS Hosseini, A Gol and M Khaleghi. The effects of *Lactobacillus acidophilus* ATCC 4356 on the oxidative stress of the reproductive system in

diabetic male rats. *International Journal of Reproductive BioMedicine* 2019; **17(7)**, 493-502.

[25] Y Umidakhon, B Erkin, G Ulugbek, N Bahadir and A Karim. Correction of the mitochondrial NADH oxidase activity, peroxidation and phospholipid metabolism by haplogenin-7-glucoside in hypoxia and ischemia. *Trends in Sciences* 2022; **19(21)**, 6260.

[26] M Bello and JA Morales-Gonzalez. Molecular recognition between potential natural inhibitors of the Keap1-Nrf2 complex. *International Journal of Biological Macromolecules* 2017; **105**, 981-992.

[27] O Trott and AJ Olson. AutoDock Vina: Improving the speed and accuracy of docking with a new scoring function, efficient optimization, and multithreading. *Journal of Computational Chemistry* 2010; **31(2)**, 455-461.

[28] T Zhang, S Zhong, L Hou, Y Wang, X Xing, T Guan, J Zhang and T Li. Computational and experimental characterization of estrogenic activities of 20(S, R)-protopanaxadiol and 20(S, R)-protopanaxatriol. *Journal of Ginseng Research* 2020 **44(5)**, 690-696.

[29] Y Leng, L Ren, S Niu, T Zhang and J Zhang. *In vitro* and *in silico* investigations of endocrine disruption induced by metabolites of plasticizers through glucocorticoid receptor. *Food and Chemical Toxicology* 2021; **155**, 112413.

[30] A Daina, O Michielin and V Zoete. SwissADME: A free web tool to evaluate pharmacokinetics, drug-likeness and medicinal chemistry friendliness of small molecules. *Scientific Reports* 2017; **7**, 42717.

[31] I Muegge. Selection criteria for drug-like compounds. *Medicinal Research Reviews* 2003; **23(3)**, 302-321.

[32] S Tian, J Wang, Y Li, D Li, L Xu and T Hou. The application of *in silico* drug-likeness predictions in pharmaceutical research. *Advanced Drug Delivery Reviews* 2015; **86**, 2-10.

[33] H Li, S Zhang and Y Zhang. Identification and quantification of bioactive compounds in Rhodiola heterodonta by HPLC. *Journal of Chromatography B* 2015; **997**, 32-40.

[34] M Gargouri, MB Salem and F Limem. Alloxan-induced diabetes in rats leads to increased lipid peroxidation and decreased superoxide dismutase activity in the liver. *Biochemical and Biophysical Research Communications* 2016; **470(4)**, 937-942.

[35] AV Mahmudov, OS Abduraimov, SB Erdonov, UG Gayibov and LY Izotova. Bioecological features of nigella sativa L. in different conditions of Uzbekistan. *Plant Science Today* 2022; **9(2)**, 421-426.

[36] UG Gayibov, EJ Komilov, RN Rakhimov, NA Egashev, NG Abdullajanova, MI Asrorov and TF Aripov. Influence of new polyphenol compound from Euphorbia plant on mitochondrial function. *The Journal of Microbiology, Biotechnology and Food Sciences* 2019; **8(4)**, 1021-1025.

[37] UG Gayibov, SN Gayibova, MK Pozilov, NA Ergashev and TF Aripov. Influence of quercetin and dihydroquercetin on some functional parameters of rat liver mitochondria. *Journal of microbiology, biotechnology and food sciences* 2021; **11(1)**, e2924.

[38] TF Aripov, UG Gayibov, SN Gayibova, AA Abdullaev, DS Abduazimova, NS Berdiev, JF Ziyavitdinov, YI Oshchepkova and SH Salikhov. Antiradical and antioxidant activity of the preparation “Rutan” from Rhus coriaria L. *Journal of Theoretical and Clinical Medicine*. 2023; **4**, 164-170.